

## Predominant Activation of JAK/STAT3 Pathway by Interleukin-6 Is Implicated in Hepatocarcinogenesis<sup>1,2</sup>

In Hye Jung<sup>\*</sup>, Jeffrey Hyun-Kyu Choi<sup>†</sup>,  
Yong-Yoon Chung<sup>‡</sup>, Ga-Lam Lim<sup>\*</sup>,  
Young-Nyun Park<sup>§</sup> and Seung Woo Park<sup>\*</sup>

<sup>\*</sup>Department of Internal Medicine, Institute of Gastroenterology, Yonsei University College of Medicine, Seoul, Korea; <sup>†</sup>Boston University College of Art and Science, Boston, MA, USA; <sup>‡</sup>Research Institute of SMT Bio, SMT Bio Co., Ltd. Seoul, Korea; <sup>§</sup>Department of Pathology, Yonsei University College of Medicine, Seoul, Korea

### Abstract

Chronic inflammation is an important process leading to tumorigenesis. Therefore, targeting and controlling inflammation can be a promising cancer therapy. Inflammation is often caused by a variety of inflammatory cytokine such as the interleukin (IL)-6, a pleiotropic cytokine known to be involved in the tumorigenesis. In this study, an *in vivo* hepatic tumorigenesis model of zebrafish was generated to demonstrate a direct consequence of the human IL6 expression causing hepatocarcinogenesis. To do this, an elevated expression of the hIL6 gene was established to specifically target the zebrafish hepatocytes by transgenesis. Interestingly, the elevated hIL6 expression caused the chronic inflammation which results in a massive infiltration of inflammatory cells. This eventually resulted in the generation of various dysplastic lesions such as clear cell, small cell, and large cell changes, and also eosinophilic and basophilic foci of hepatocellular alteration. Hepatocellular carcinoma was then developed in the transgenic zebrafish. Molecular characterization revealed upregulation of the downstream components involved in the IL6-mediated signaling pathways, especially PI3K/Akt and JAK/STAT3 pathways. Further investigation indicated that PI3K was the most reactive to the infiltrated inflammatory cells and dysplasia with large cell change, whereas STAT3 was heavily activated in the region with dysplastic foci, suggesting that the JAK/STAT3 pathway was mainly implicated in the hepatic tumorigenesis in the current model. Our present study provides an *in vivo* evidence of the relationship between chronic inflammation and tumorigenesis and reinforces the pivotal role of IL6 in the inflammation-associated hepatocarcinogenesis.

*Neoplasia* (2015) 17, 586–597

### Introduction

The liver is the largest internal organ and plays a major role in the systemic metabolism of humans. The organ must not only be able to produce biochemicals necessary for digestion, it must also be able to protect against damage by the ingested agents, such as drugs [1]. Hepatic immune system is very important to identify, detoxify, and also neutralize pathogens, and failure of this immune system can cause the chronic inflammation which leads to hepatocarcinogenesis. Chronic inflammation can induce alteration of the specific signaling pathways involved in cell proliferation and survival during hepatic regeneration, increasing risk of hepatocellular carcinogenesis. Among the various substances present in the inflammation process, interleukin (IL)-6 has been proven to have a crucial role in hepatocellular carcinoma (HCC) [2].

Abbreviations: IL6, interleukin-6; JAK, Janus kinase; STAT3, signal transducer and activator of transcription 3; PI3K, phosphoinositide 3-kinase; MAPK, mitogen activated protein kinase; LFABP, liver fatty acid binding protein; RS6K, ribosomal S6 kinase; HCC, hepatocellular carcinoma; dpf, days post-fertilization  
Address all correspondence to: Seung Woo Park, Yonsei-Ro 50-1, Seodaemun-Gu, Seoul, Korea 120-140.

E-mail: [swoopark@yuhs.ac](mailto:swoopark@yuhs.ac)

<sup>1</sup> Funding: This study was funded by National Research Foundation of Korea (Basic Science Research Program, 7-2012-0531) and Korea Health Industry Development Institute (KHIDI, Research-Oriented Hospital Program, HI14C1324).

<sup>2</sup> Conflict of interest: None declared.

Received 6 May 2015; Revised 4 July 2015; Accepted 13 July 2015

© 2015 The Authors. Published by Elsevier Inc. on behalf of Neoplasia Press, Inc. This is an open access article under the CC BY-NC-ND license (<http://creativecommons.org/licenses/by-nc-nd/4.0/>).

1476-5586

<http://dx.doi.org/10.1016/j.neo.2015.07.005>

IL6 is a highly versatile cytokine which was originally characterized as the regulator that stimulates the final maturation of B cell [3]. This cytokine is also known to promote hepatic survival by stimulating liver regeneration [4–6]. Upon binding of IL6 to its receptor, glycoprotein 130, the receptor is phosphorylated by Janus kinase (JAK) and in turn induces multiple signaling pathways, including JAK/STAT3, PI3K/Akt, and Ras/Raf/MAPK pathways [7]. These pathways have a fundamental role in the hepatic regeneration by blocking and reducing apoptotic cascade and oxidative injury [7–9]. A rapid transition from quiescence into cell cycle of the hepatocytes is thus a part of the hepatic regeneration process. These suggest that IL6 is an important mediator of the hepatocyte regeneration and functions as a critical proregenerative factor and acute-phase inducer in liver injury.

In contrast, growing evidences indicating that IL6 level is elevated in various cancer tumorigenesis associated with the chronic inflammation have been reported: Inappropriately high level of the IL6 production has been detected in breast cancer mammospheres [10]. A non-small-cell lung adenocarcinoma has also provided additional evidence for the involvement of IL6 in tumorigenesis [11]. These reports raise the question of whether the elevated cytokine level is implicated in inflammation and tumorigenesis. In fact, a previous study showed that a high level of IL6 expression rather inhibits liver regeneration by increasing expression of the p21, the cyclin-dependent kinase inhibitor [12]. The results suggest that IL6 possesses both pro- and antimitogenic actions and that its signaling process might be regulated by a negative feedback loop.

In the past decade, zebrafish has been used as an experimental model for human diseases, including human liver cancer [13–15]. Zebrafish and humans share the molecular and cellular conservation at various levels in tumorigenesis, indicating the potential of zebrafish for modeling human cancer [16]. In the present study, we have generated and validated a novel transgenic zebrafish model demonstrating an elevated expression of the human IL6 gene specifically in the liver. Investigation of the transgenic zebrafish showed typical features of inflammation-associated dysplasia and HCC in human. Further characterization at molecular and cellular levels revealed that the hIL6-induced hepatic tumorigenesis was mediated by JAK/STAT3 signaling pathway. This report discusses the *in vivo* evidence that hepatic expression of the hIL6 induces the chronic inflammation leading to hepatocarcinogenesis.

## Materials and Methods

### Transgene Constructs and Transgenesis

All constructs used in our study were sequenced and verified using the appropriate primers listed in Supplementary Table S1. For transgenesis, the transgene constructs p(LFABP:Gal4VP16), p(UAS:RFP), and p(UAS:hIL6,Cmcl2:GFP) were separately generated (Figure 1A). Briefly, a 2.8-kb upstream region of the liver-specific LFABP gene was polymerase chain reaction (PCR)-amplified as referenced by a previous report [17] and used as the promoter to drive Gal4VP16 gene in the zebrafish liver. The hIL6 cDNA purchased from Open Biosystems (Huntsville, AL) was PCR-amplified and cloned into the downstream of UAS promoter. Then, Cmcl2-GFP (for cardiac expression of GFP) was PCR-amplified and cloned to generate p(UAS:hIL6,Cmcl2:GFP). The p(UAS:RFP) was prepared by placing the RFP sequence amplified from pAsRed2 (Invitrogen, Carlsbad, CA) under the pUAS promoter. Refer to Supplementary Table 1 for primer sequences.

For microinjection, each injection mixture was prepared by reconstituting Tol2-transposase mRNA with the transgene constructs p(LFABP:Gal4VP16) with p(UAS:RFP) and p(UAS:hIL6,Cmcl2:GFP) separately in the Danieus buffer mixed with 0.03% phenol red. The injection mixture was then introduced into the yolk of embryos using an MMPI-2 microinjector at single-cell stage of AB embryos. F0 founder embryos were selected under a fluorescence microscope (Olympus, Japan) based on RFP in the liver and cardiac GFP expression. The zebrafish were bred to give a birth to the F1 strains *Tg(LFABP:Gal4VP16;UAS-RFP)* and *Tg(UAS:hIL6,Cmcl2:GFP)*. By crossing these two *Tg* strains, the transgenic zebrafish expressing hIL6 specifically in the liver, i.e., *Tg(LFABP:Gal4VP16;UAS-RFP;UAS:hIL6,Cmcl2:GFP)*, was established (Figure 1C). We found that all transgenes were transmitted in normal Mendelian ratio.

### Animal Stocks and Embryo Care

All zebrafish were raised in a standardized aquaria system (Genomic Design Co., Daejeon, Korea) (<http://zebrafish.co.kr>). The system provides continuous water flow, biofiltration tank, constant temperature maintenance at 28.5°C, UV sterilization, and 14-hour light and 10-hour dark cycle. The genetic strain of the zebrafish used in this study was the AB line purchased from Zebrafish International Resource Center (ZIRC, Eugene, OR) (<http://zebrafish.org>). Embryos to be processed for whole-mount analyses were placed in an E3 medium with 0.003% phenylthiourea at 24 hpf to inhibit pigmentation. We strictly followed the Guidelines for the Welfare and Use of Animals in Cancer Research [18].

### Histology, Immunohistochemistry (IHC), and In Situ Hybridization (ISH)

Histologic evaluation was done by preparing 4- $\mu$ m transverse sections from 4% paraformaldehyde-fixed, paraffin-embedded tissue. Hematoxylin and eosin (H&E) staining was performed according to the standard protocol [19]. IHC and ISH experiments were carried out as previously described [20]. Primary antibodies in the experiments were rabbit anti-IL6 (1:200), rabbit anti-caspase 3 (1:100), mouse anti-proliferating cell nuclear antigen (PCNA) (1:2000), and rabbit anti-JAK1 (1:200) from Abcam (Cambridge, MA). Mouse anti-phospho-PI3K (1:100) was purchased from Santa Cruz Biotechnology, Inc. (Santa Cruz, CA). Rabbit antibodies for phospho-Tuberin/TSC2 (1:200), phospho-mTOR (1:200), phospho-4EBP1 (1:200), phospho-RS6K (1:200), and phospho-STAT3 (1:200) were purchased from Cell Signaling (Danvers, MA). For ISH experiment, partial cDNA sequences were PCR-amplified using the appropriate primers (refer to Supplementary Table 2) and cloned into pCRII vector (Invitrogen). Riboprobes were generated using T7 or SP6 digoxigenin labeling kit (Roche Diagnostics GmbH, Mannheim, Germany). Hybridization was done at 65°C overnight, and a series of stringent wash was done at 68°C. Hybridized riboprobes were detected by anti-dig antibody binding and visualized by incubating with an NBT/BCIP AP substrate solution (Roche Diagnostics GmbH). Counterstaining was done with neutral red.

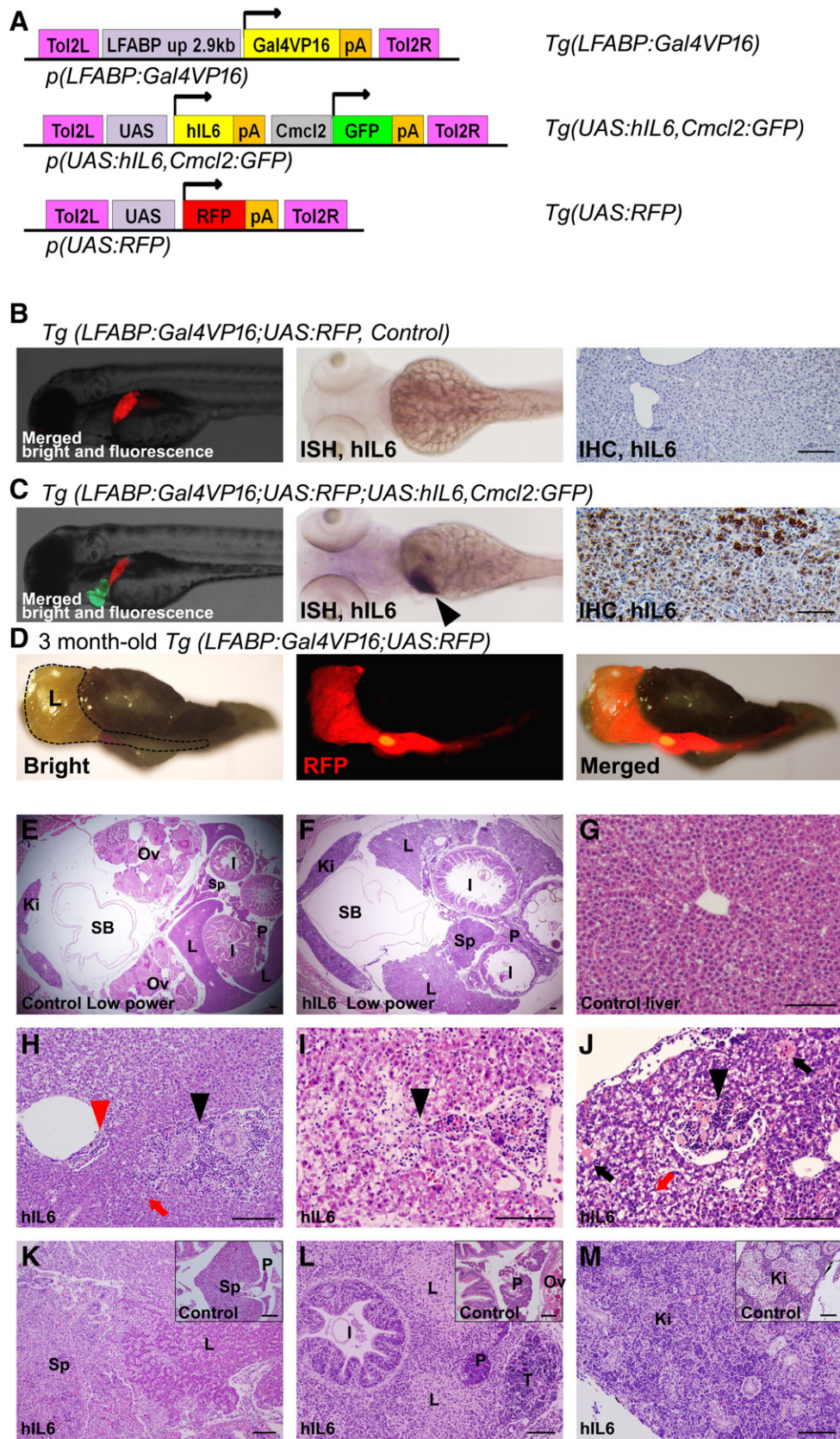
### Imaging

Olympus MVX10 was used for whole-mount embryo imaging. Photographs from slide sections were obtained using an Olympus BX51.

### Reverse transcriptase (RT)-PCR and Western Blot Analyses

Real-time RT-PCR was performed by using the whole liver tissue dissected from 3-month-old zebrafish. For each group, RNA sample was





extracted by using TRIzol reagent (Invitrogen). cDNA was synthesized by using a Maxima First Strand cDNA Synthesis Kit (Thermo Scientific Fermentas, K1641, Glen Burnie, MD). The RT-PCR was performed by using Maxima SYBR Green/ROX qPCR Master Mix (Thermo Scientific Fermentas, K0222) on a 7300 Real-Time PCR System

(Applied Biosystems, Foster city, CA). Primer sequences for the RT-PCR are shown in Supplementary Table 3. All experiments were repeated three times with individually prepared samples. Statistical significance was analyzed by the Mann-Whitney *U* test using SPSS 11 software. For Western blot assay, whole cell extracts were prepared from

zebrafish liver as described previously [21]. Twenty micrograms of each sample was separated on a 10% SDS–polyacrylamide gel and transferred onto a polyvinylidene difluoride membrane (Amersham, GE Health, Sweden). The membrane was incubated overnight at 4°C with primary antibody in a PBS blocking solution (nonfat dry milk). Horseradish peroxidase–conjugated secondary antibody was used for post reaction. Labeled proteins were then detected by ECL reagents and Hyperfilm ECL (Amersham Biosciences).

### Inhibition Assay on IL6-Mediated Pathway

To block the hIL6-mediated downstream signaling in live zebrafish, the two STAT3 inhibitors, Niclosamide (S3030; Selleckchem; IC50 0.7  $\mu$ M) and Stattic (S7024; Selleckchem; IC50 5.1  $\mu$ M), were used. BKM 120 (sc-364437; Santa Cruz Biotechnology) was used for inhibiting the downstream molecules of PI3K pathway (IC50 for p110 $\alpha$ , p110 $\beta$ , p110 $\gamma$ , and p110 $\delta$  with 52 nM, 166 nM, 262 nM, and 116 nM, respectively). To determine treatment doses, 6-week-old juvenile zebrafish were treated with a serial escalation of each inhibitor for 7 days. Maximal tolerable doses (MTDs), i.e., the highest concentration that caused no more than 25% fatality (100 nM for BKM120, 0.3  $\mu$ M for Niclosamide, and 1  $\mu$ M for Stattic), were used for the treatment. For short-term treatment, the 6-week-old zebrafish divided into four groups were treated with the MTDs for 10 days and then were processed for liver dissection and RT-PCR experiment. For chemoprevention analyses, the same groups (20 per each group) were separately treated with each inhibitor in 1-l water tank for 6 weeks and then were processed for histologic analyses.

## Results

### Chronic Inflammation Induced by Sustained Expression of hIL6 in Zebrafish Liver

We have generated transgenic zebrafish lines to demonstrate hIL6-driven tumorigenesis. To do this, independent transgenic lines of *Tg(UAS:hIL6,Cmcl2:GFP)* were established and crossed with *Tg(LFABP:Gal4VP16;UAS:RFP)* (Figure 1A). We found that binary expression by the Gal4-UAS system has allowed the liver specific expression of the transgenes in the zebrafish (Figure 1, B–D). RFP expression and ISH analyses confirmed that the transgene expression was apparently detected in the zebrafish liver from 4 days postfertilization (dpf) and persisted until adulthood. IHC experiment against the hIL6 with the liver section also confirmed the hIL6 expression in the hepatocytes (Figure 1C). By selecting the transgenic lines under a fluorescence microscope, heterozygote zebrafish were maintained and used for all experiments.

We conducted microscopic observations with the liver sections from the transgenic zebrafish (Figure 1, E–M) and found that the zebrafish liver appeared to contain various grades of inflammatory cell infiltration in all of the transgenic zebrafish expressing the hIL6. The results showed that the inflammatory cell infiltration was often detectable in portal areas, hepatic sinusoids, and intrahepatic vessels (Figure 1, H–J). We also found that the inflammatory cell infiltration occurred in the adjacent organs including pancreas, intestine, spleen, and kidney (Figure 1, K–M). The inflammatory changes was classified as low grade or high grade depending on the degree of inflammatory cell infiltration and organ destruction: Histologically, low grade shows a predominant infiltration of the inflammatory cells in the liver with scanty or mild infiltration into the neighboring organs, still preserving the liver architecture, whereas high grade shows a massive infiltration of the inflammatory cells into both liver and its adjacent organs, destructing the organ architecture (Figure 1, K–M). We found that high grade of the inflammatory change was in one third (Table 1). We assumed that severe local inflammation in the liver induced the systemic effect which results in the inflammation in the hematopoietic and lymphoid organs (kidney and spleen, respectively). Likely, the severe local inflammation ran off from the liver into the adjacent organs and caused inflammation in the pancreas and intestine because of the close proximity between the liver and these internal organs in zebrafish. Taken together, the results suggest that the sustained expression of hIL6 has induced chronic inflammation in the transgenic zebrafish liver.

### Hepatocellular Tumorigenesis with Multiple Foci of Dysplasia Appeared in the hIL6-Expressing Zebrafish Liver

During the course of hepatic tumorigenesis in mouse model, different types of dysplastic foci have appeared before HCC [22]. Similarly, we found that various hepatocellular changes began to occur in the transgenic zebrafish liver at 2 months of age, including clear cell, small and large cell, and eosinophilic and basophilic cell foci (Figure 2, A–F). Increased cell density and variable degree of cellular and nuclear pleomorphism were observed. (Figure 2, E–G). Large cell change with both nuclear pleomorphism and megalocytosis was notably detected (Figure 2H). Multinucleated cells and the cytoplasm containing eosinophilic multilamellarlike structures were frequently found (Figure 2, H and I). We found that most of the dysplastic foci that occurred in the liver were accompanied by variable degree of inflammatory changes. Dysplastic foci, however, occasionally developed in the liver with scanty inflammation of surrounding area (Figure 2B). Occasionally, the dysplastic foci became larger, forming a

**Figure 1.** Transgenic strategy and specific expression of hIL6 gene in transgenic zebrafish. (A) Structure of the constructs used in the Tol2-mediated transgenesis. (B and C) Embryo images at 4 dpf (left, merged images) showed RFP expression in the liver. Hepatic expression of RFP and cardiac expression of GFP were used as the indicators to select the transgenic embryos under a fluorescence microscope. ISH for hIL6 (middle) at 4 dpf showed its RNA expression in the liver (black arrowhead). IHC at 6 weeks (right) showing the hIL6 expression at the hepatocytes only in *Tg(LFABP:Gal4VP16;UAS:RFP;UAS:hIL6,Cmcl2:GFP)*. (D) A whole dissected viscera at 3 months showing the liver-specific expression of RFP. Dotted line indicates liver boundary. (E and F) Low-power images at 2 months. Note that the liver surface of the hIL6-expressing transgenic fish shows irregular contour due to inflammation. (G) H&E image of control liver at 6 weeks of age showing normal architecture with central vein at the center of image. (H–J) H&E images of the hIL6-expressing zebrafish showing the infiltration of inflammatory cells in the liver at 6 weeks of age. (H) Infiltration of the inflammatory cells was noted at a portal and a perivascular area (black and red arrowheads, respectively). Feathery degeneration (red arrow) is seen. (I) Inflammatory cells at hepatic sinusoids (black arrowhead). Pale to clear cytoplasm suggests ballooning degeneration of hepatocytes. (J) Inflammatory cells in an intrahepatic vessel (black arrowhead) are noted. Spotty necrosis (black arrows) and feathery degeneration (red arrow) are noted. (K–M) Three-month-old zebrafish. (K) Severe inflammation caused enlargement of spleen and adhesion to the liver (inset, control spleen). (L) Destructive change causing adhesion of liver, pancreas, intestine, and testis (inset, control pancreas). Swollen hepatocytes with pale cytoplasm indicate ballooning degeneration of the hepatocytes. (M) Inflammatory cell infiltration in the kidney (inset, control kidney showing hematopoietic cells between renal tubules). Ki, kidney; I, intestine; L, liver; Ov, Ovary; P, pancreas; SB, swim bladder; Sp, spleen; T, testis. Bars, 50  $\mu$ m.



discrete nodule which mimics the dysplastic nodule occurring in the hepatic tumorigenesis of human (Figure 2Q). The histopathological analysis revealed that the transgenic zebrafish liver harbors multiple foci of dysplasia, indicating that the tumorigenic process polyclonally occurred in multiple areas (Figure 2A). Further investigation revealed that the dysplastic foci developed in almost all transgenic zebrafish at 3 months, showing near 100% penetrance. In an attempt to count the number of the dysplastic foci, we prepared serial section slides at 0.5-mm interval for observation of the whole liver. The numbers of the dysplastic foci were  $4.5 \pm 1.6$ ,  $7.1 \pm 2.1$ , and  $6.6 \pm 1.9$  at 3, 6, and 9 months, respectively ( $P > .05$ ) (Table 1). Among the dysplastic foci, clear cell foci were found to be the most predominant as it comprised 52.4%, which is followed by large cell foci (32.1%), small cell foci (10.9%), eosinophilic cell foci (3.2%), and basophilic cell foci (1.4%) (Table 1).

We performed IHC experiments for hIL6 to see whether the tumor cells in the dysplastic focus express the transgene (Figure 2, M–O). Expression of PCNA as a prognostic indicator [23] to demonstrate the enhanced cellular proliferation during the liver tumorigenesis was also investigated (Figure 2, P–R, Supplementary Figure 1). The results showed that the hepatocytes at the dysplastic foci showed a higher level of positivity to hIL6 and PCNA expressions, suggesting that the dysplasia was caused by the direct consequence of the elevated hIL6 expression. The enhanced cell proliferation often contributed to form the discrete nodule (Figure 2Q). Eventually, we found that approximately 12.5% (3/24) and 16.7% (4/24) of the hIL6-expressing liver contained typical features of HCC at 6 and 9 months of age, respectively (Table 1). The typical features included severe nuclear and cytological pleomorphism, prominent nucleoli, and frequent mitosis in the lesions. Although frank invasion into the adjacent organs was not found, occasional tumor thrombi were noted in intrahepatic vessels (Figure 2L). Taken together, the results suggested that the hIL6-expressing transgenic zebrafish has developed HCC through the formation of dysplastic foci.

### Upregulation of Inflammatory and Carcinogenic Pathways Driven by the Elevated Expression of hIL6

Understanding the signaling pathway that mediates the inflammatory tumorigenesis is important for the identification of novel therapeutic targets for HCC. Upon binding of IL6 to its receptor, the pleiotropic effects of IL6 appear through JAK/STAT3 and PI3K/Akt pathways during hepatic inflammatory tumorigenesis [24–26]. These

pathways are also implicated in tumor cell survival by regulating antiapoptotic genes [27]. Another important signaling pathway is Ras-Raf-MAPK pathway, which also transduces signals for cell growth, division, and differentiation [28].

To see the molecular regulation induced by the aberrant expression of hIL6, we selected a list of the genes that might be modulated in the IL6-mediated pathways and performed RT-PCR experiments (primers are listed in Supplementary Table 2). The result revealed that the elevated expression of hIL6 induced upregulation of the various components involved in the signaling pathways by many folds (Figure 3). Among these, the most prominent expression change was detected from c-Myc, known as a cell growth regulator [29] (Figure 3A). Cell survival and cell cycle regulators MAPK1 and cyclin D1 were also shown to be upregulated. The results suggest that enhanced hepatocellular proliferation has been induced by the elevated hIL6 expression. IL1b and IL12a were used as the indicators for inflammatory response, and the RT-PCR showed that these components were also upregulated, suggesting that hepatic inflammation has been activated in the transgenic zebrafish liver (Figure 3A). Aberrant activation of the IL6-induced JAK/STAT3 pathways was noticed from the RT-PCR of their downstream components such as c-Myc, Appa, Socs, Pim1, and Cis. The activation of PI3K/Akt pathway was also evident by upregulation of Xiap and Eif1a.

Further confirmation of our findings in the RT-PCR results was obtained from Western blot experiment (Figure 3B). We found that the phosphoproteins of the major signaling pathways, pMAPK, pPI3K, and also pSTAT3, were abundantly present in the transgenic zebrafish liver, suggesting that the all downstream signaling pathways of IL6 were activated. Taken together, our results strongly support that HCC development in the transgenic zebrafish is caused by the elevated expression of hIL6.

### Predominant Activation of JAK/STAT3 Pathway Is Involved in the IL6-Mediated Tumorigenesis

To find further insights into the molecular mechanism of the HCC development caused by hIL6, we evaluated the downstream molecules at histological level by IHC and ISH analyses (Figures 4 and 5, Supplementary Figures 1 and 2). Antibody against active caspase 3 was frequently reactive to the hepatocytes expressing hIL6, indicating that the hIL6-mediated chronic inflammation has induced cell death (Figure 4B). The chronic inflammation inevitably resulted in the cell damage followed by regenerative cell renewal and

**Table 1.** Histopathological Changes by hIL6 Expression in Hepatocytes

	<i>Tg(LFABP:Gal4VP16;UAS:RFP)</i>	<i>Tg(LFABP:Gal4VP16;UAS:RFP;UAS:hIL6,Cmcl2:GFP)</i>			
	Control ( <i>n</i> = 24) (8 Zebrafish at 3, 6, and 9 Months)	3 Months ( <i>n</i> = 24)	6 Months ( <i>n</i> = 24)	9 Months ( <i>n</i> = 24)	Sum ( <i>n</i> = 72)
<b>Hepatic inflammation</b>	<b>1 (3.3%)</b>	<b>100%</b>	<b>100%</b>	<b>100%</b>	<b>100%</b>
Low	1 (3.3%)	16 (66.7%)	15 (62.5%)	17 (70.8%)	48 (66.7%)
High	None	8 (33.3%)	9 (37.5%)	7 (29.2%)	24 (33.3%)
<b>Dysplastic foci</b>	<b>None</b>	<b>100% <i>n</i> = 108 (4.5 ± 1.6/fish)</b>	<b>100% <i>n</i> = 173 (7.2 ± 2.1/fish)</b>	<b>100% <i>n</i> = 158 (6.6 ± 1.9/fish)</b>	<b>100% <i>n</i> = 439 (6.1 ± 1.8/fish)</b>
Clear cell foci		54 (50.0%)	90 (52.0%)	86 (54.4%)	230 (52.4%)
Large cell foci		38 (35.2%)	57 (32.9%)	46 (29.1%)	141 (32.1%)
Small cell foci		11 (10.2%)	17 (9.8%)	20 (12.7%)	48 (10.9%)
Eosinophilic cell foci		3 (2.8%)	6 (3.5%)	5 (3.2%)	14 (3.2%)
Basophilic cell foci		2 (1.9%)	3 (1.7%)	1 (0.6%)	6 (1.4%)
<b>HCC</b>	<b>None</b>	<b>0 (0%)</b>	<b>3 (12.5%)</b>	<b>4 (16.7%)</b>	<b>8 (8.9%)</b>

Statistical difference was not found in the number of dysplastic foci or in types according to the month-age of transgenic zebrafish.

proliferation. Expression of the proliferation markers PCNA, pMAPK, and cyclin D1 was abundantly detected in the liver with dysplastic and nondysplastic foci, indicating that the regeneration process has been largely triggered by the elevated IL6 expression in the liver (Figure 4, D, F, and H). Lineage analyses of the infiltrated inflammatory cells were performed by ISH with leukocyte markers. We found that abundant CD4-positive T cells were observed in the portal tracts with occasional CD8-positive cells at hepatic parenchyma (Figure 4, J and L). Ighm-positive B cells and Spi1-positive myeloid cells were also observed at hepatic sinusoids and portal area (Figure 4, N and P). These findings suggested that the hIL6-induced chronic inflammation accompanied nonspecific recruitment of the lymphoid and myeloid lineage cells.

Because both phospho-PI3K and phospho-STAT3, the major regulators of IL6 signaling pathway, were shown to be activated in the tumorigenic zebrafish liver (Figure 3), IHC was performed to further delineate the inflammation-induced tumorigenesis at the histologic level (Figure 5). Interestingly, we found that pPI3K expression was largely restricted to the infiltrated inflammatory cells but not to the dysplastic foci (Figure 5A and Supplementary Figure 2). Among the various dysplastic foci, only the cells with large cell change were prominently reactive to the pPI3K immunostaining (Figure 5B and Supplementary Figure 2). Similarly, the downstream components of PI3K such as pAkt1, pRS6K, pTuberin, and p4EBP1 were shown to be positive to the hepatocytes with large cell change but not to the other dysplastic and HCC cell (Figure 5, C–F). The IHC experiment using the serial sections of the zebrafish liver with large cell change also showed a predominant activation of the molecular components in the PI3K pathway (Supplementary Figure 2). The results suggest that the PI3K/Akt pathway is the most reactive to the inflammatory cell and large cell change and is not primarily involved in the IL6-induced tumorigenesis.

Hepatocellular immunostaining to identify pSTAT3 was also done (Figure 5 and Supplementary Figure 1). The result showed that virtually all of the hepatocytes expressing hIL6 were reactive to pSTAT3 and that the pSTAT3 expression heavily occurred in the region with dysplastic foci (Figure 5, G–I and Supplementary Figure 1). Unlike the pPI3K expression, however, we found that the infiltrated inflammatory cells were negative to the pSTAT3 staining (Figure 5, G–I). ISH experiments for the downstream molecules of JAK/STAT3 signaling pathway such as Socs, Appa, Cis, and Pim1 revealed that the genes were strongly expressed in the dysplastic region which was reactive to pSTAT3 immunostaining (Figure 5, J–O). Expression analysis with serial sections of the zebrafish liver corroborated the enhanced activation of STAT3 pathway (Supplementary Figure 1). Taken together, our results suggest that activation of JAK/STAT3 pathway in hepatocytes is primarily responsible for IL6-mediated hepatic tumorigenesis.

#### Drug Inhibition of the IL6-Mediated Signaling Pathways

Our molecular and cellular analyses indicated that the IL6-mediated JAK/STAT3 pathway was a key signal transduction pathway implicated in the hepatic tumorigenesis. Evaluation of inhibition efficacy of the JAK/STAT3 pathway would further reveal that the signaling pathway is mainly responsible for the tumor development. Inhibition assay of the PI3K/Akt pathway would also support that the pathway is involved in the IL6-mediated hepatic inflammation. To elucidate, two STAT3 inhibitors (Niclosamide and Stattic) and a PI3K inhibitor (BKM120) were administered to the transgenic zebrafish, and their downstream

components were investigated at the molecular and cellular level (Figure 6). Real-time RT-PCR performed after 10 days with the inhibitor treatment indicated that Niclosamide and Stattic showed modest inhibition of JAK/STAT3 pathway, whereas BKM120 was not effectively reactive to the PI3K inhibition (Figure 6A). The results suggested that the drug inhibition partially worked in the JAK/STAT3 pathway.

Histologic evaluation was also performed by H&E and IHC after 6 weeks of the treatment, a long-term treatment. We found that BKM120 showed the decreased immunoreactivity to pPI3K in the inflammatory cells (Figure 6B), supporting our present finding of the PI3K/Akt pathway which is involved more likely in the inflammatory process. The STAT3 inhibitors revealed variable effect on the expression of downstream genes, i.e., decreased expression was noted for Appa but others on ISH (Figure 6F). Likely, the pSTAT3 or PCNA immunoreactivity in the hepatocytes was not inhibited by either Niclosamide or Stattic, suggesting that the inhibitors did not completely suppress the JAK/STAT3 pathway (Figure 6, C and D). Nonetheless, identification of the PCNA positivity correlated with the pSTAT3 expression at the same tissue section (Figure 6, B–D, red circles), suggesting that activation of the JAK/STAT3 pathway is responsible for IL6-mediated tumorigenesis.

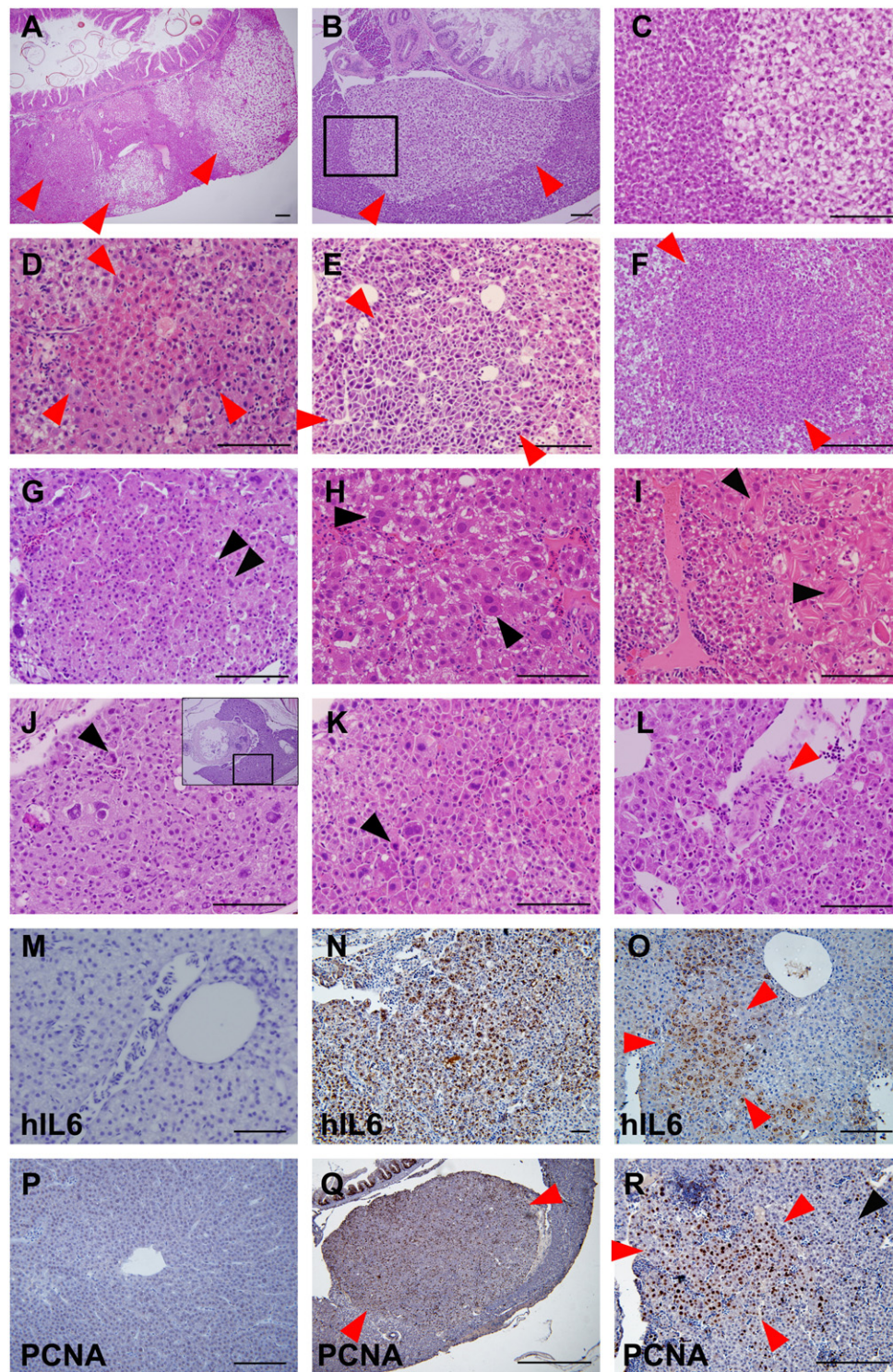
Likely, the counted numbers of the dysplastic foci were  $3.3 \pm 1.1$ ,  $2.7 \pm 0.9$ ,  $3.1 \pm 1.0$ , and  $3.0 \pm 1.1$  in control, BKM120, Niclosamide, and Stattic treatment groups, respectively ( $P > .05$ ). This seemed to be caused by dose-limiting toxicity of the inhibitors: We found a treatment toleration with BKM120 at the concentration of 100 nM (comparable to the concentration of IC50), whereas the zebrafish were poorly tolerable to Niclosamide (MTD 0.3  $\mu$ M, which is lower than IC50 of 0.7  $\mu$ M) and Stattic (MTD 1  $\mu$ M, which is lower than IC50 of 5.1  $\mu$ M).

#### Discussion

In the present study, we have introduced the hIL6 gene into zebrafish to investigate if the elevated hIL6 expression causes hepatocellular tumorigenesis in the liver. IL6 is a well-known cytokine playing a crucial role in liver regeneration and also hepatic tumorigenesis depending on its expression condition [4–6,11]. Under normal circumstances, the inflammation-associated expression of IL6 might have a protective role of hepatocyte death. Inappropriate or uncontrolled expression of this pleiotrophic cytokine, however, can be detrimental to the liver, causing accentuation of inflammatory process, cell damage and death, and eventually generation of HCC. In our study, we observed that the zebrafish containing the elevated expression of hIL6 gene specifically in the liver caused the chronic inflammation which results in a massive infiltration of inflammatory cells (Figure 1). Detailed microscopic investigation of the liver showed that the transgenic zebrafish liver developed typical features of HCC with dysplastic foci, suggesting that the elevated expression of hIL6 caused hepatocellular tumorigenesis (Figure 2).

IL6 acts through multiple signal transduction pathways [4,8,10]. Among the pathways, JAK/STAT3 plays very important roles in inflammation and tumorigenesis. STAT3 belongs to the STAT protein family consisting of seven members and is especially known to be a key element in tumor initiation and progression [30,24]. Normal activation of the STAT3 by phosphorylation in response to IL6 leads to turn on transcriptions of many downstream genes involved in normal hepatic development, whereas abnormal persistent activation of the element contributes to tumorigenesis and chronic inflammation, suggesting that STAT3 has dual role. In our study with the





transgenic zebrafish, the elevated hIL6 expression has been shown to activate the JAK/STAT3 pathway, causing tumorigenesis. To delineate the IL6-driven hepatic inflammation and tumorigenesis, we took advantage of using different downstream markers to take insights into the molecular mechanism. Interestingly, we found that virtually all neoplastic hepatocytes are strongly reactive to STAT3 elements (Figure 5). Identification of the phospho-STAT3 protein and its downstream molecules was prominently localized in the hepatic region with dysplastic foci. The results indicated that the JAK/STAT3 pathway activated by hIL6 expression is primarily implicated in the hepatocellular tumorigenesis.

PI3K, another regulatory element in the IL6-mediated signaling, showed the most reactivity to the infiltrated inflammatory cells, and the reactivity of its downstream molecules appeared mainly on the hepatocytes with large cell change (Figure 5 and Supplementary Figure 2). Although the IL6-mediated activation of PI3K/Akt pathway may play an important role in the dysplasia with large cell changes, our findings suggested that the PI3K/Akt pathway was rather interconnected with the inflammatory process than with tumorigenesis during the IL6-mediated signaling.

Another IL6-mediated signaling is Ras/Raf/MAPK pathway [29]. In this pathway, the mitogen-activated protein kinase, pMAPK, plays

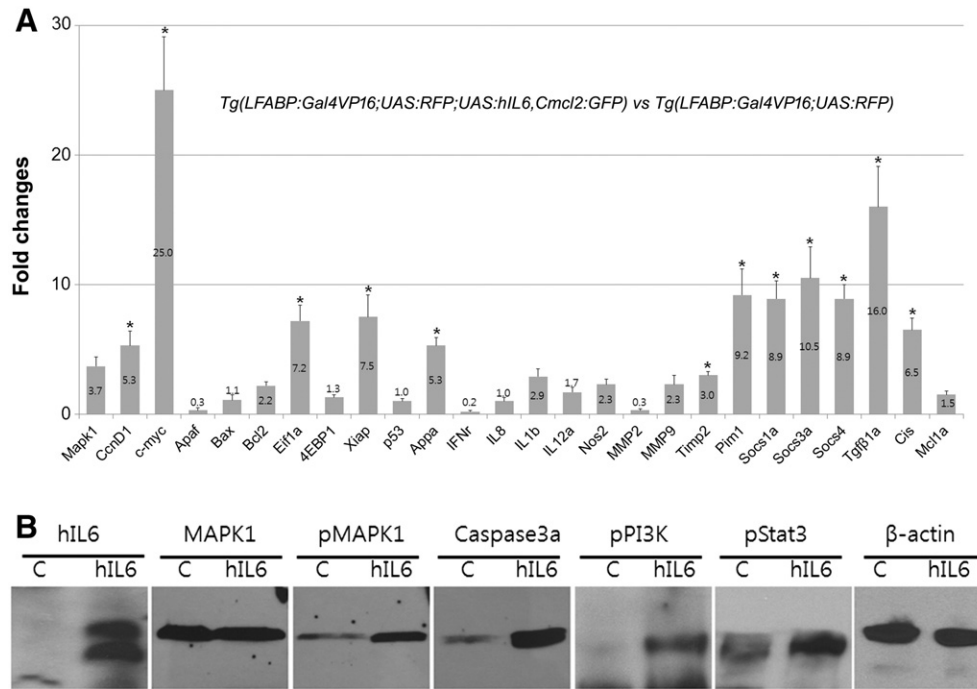


**Figure 3.** RT-PCR and Western blot analysis. Samples were prepared from the whole livers dissected under a fluorescence microscopy from 3-month-old zebrafish. (A) Real-time RT-PCR showing differential expression of the downstream components of IL6 signaling. Graphs are shown with mean value and standard error bars. Note the prominent upregulation of Myca and JAK/STAT3 downstream components. (B) Western blot hybridization showing upregulation of the active phosphorylated downstream components of IL6 signaling pathway. C, *Tg(LFABP:Gal4VP16;UAS:RFP)*. hIL6, *Tg(LFABP:Gal4VP16;UAS:RFP;UAS:hIL6,Cmcl2:GFP)*. The asterisk indicates significant difference between the hIL6-expressing group and control as determined by Mann-Whitney *U* test ( $P < .05$ ). hIL6, 26 kDa; MAPK1, 52 kDa; pMAPK1, 52 kDa; caspase 3a, 35 kDa; pPI3K, 85 kDa; pSTAT3, 86 kDa;  $\beta$ -actin, 45 kDa.

a pivotal role in cell proliferation during the inflammatory response, transducing extracellular signal to the cell nucleus, and thereby its specific genes are activated for cell growth [26]. In our RT-PCR experiment, various cellular proliferation markers were shown to be upregulated in the hIL6-expressing zebrafish liver (Figure 3). Immunostaining analysis revealed that their upregulations appeared on the hepatocytes with both dysplastic and also nondysplastic foci (Figure 4). The results indicated that the hepatocellular proliferation and regeneration process has been largely triggered by the elevated IL6 expression in the transgenic zebrafish liver. Taken together, our study revealed that the elevated IL6 expression induced inflammation and tumorigenesis and that the IL6-induced HCC was mediated mainly by JAK/STAT3 pathway.

It seems that IL6 plays a role in two different ways to cause hepatocarcinogenesis: First is the robust chronic inflammation which results in the infiltration of inflammatory cells. The chronic inflammation induces cell damage followed by the enhanced proliferation which results in the occurrence of dysplasia. Secondly, the activated JAK/STAT3 pathway itself may be sufficient enough to induce dysplasia because our findings showed that dysplastic foci still occurred in the liver with scanty inflammation in the surrounding area.

In zebrafish, several inducible models showing the features of hepatocarcinogenesis have been reported [31–36]. Induced expression of oncogenic *xmrk* gene showed a successful HCC in zebrafish [31]. Liver tumors were rapidly induced with 100% penetrance in both juvenile and adult *xmrk* transgenic fish. The authors also examined

**Figure 2.** H&E staining of liver tumor progression in the transgenic zebrafish. (A–C) Two-month-old zebrafish. (D–I, M–R) Three-month-old zebrafish. (J–L) Six-month-old zebrafish. (M) and (P) are control liver images of *Tg(LFABP:Gal4VP16;UAS:RFP)*, and others are from *Tg(LFABP:Gal4VP16;UAS:RFP;UAS:hIL6,Cmcl2:GFP)*. All red arrowheads indicate dysplastic foci. (A) Multiple foci of hepatocellular alteration (red arrowheads). Clear cell change was most frequently observed. (B) Clear cell focus with scanty inflammation in the surrounding liver. (C) A high-power observation of the boxed area of (B) showing nuclear pleomorphism. (D) Eosinophilic focus of hepatocellular alteration. (E) Basophilic cell change showing cytological atypia with nuclear pleomorphism and high nucleocytoplasmic ratio. (F) Small cell change with increased cell density and high nucleocytoplasmic ratio. (G) Small cell change showing nuclear pleomorphism and occasional multinucleation (black arrowheads). (H) Large cell change with nuclear pleomorphism and frequent multinucleated cells (black arrowheads). (I) Dysplastic changes with eosinophilic multilamellar structure (black arrowhead). (J–L) Overt HCCs showing marked nuclear and cytological pleomorphism of tumor cells at 6 (J) and 9 (K and L) months. (J) High-magnification view of boxed area of inset. Occasional mitoses are seen (black arrowheads). Occasionally, tumor cells invaded intrahepatic vessels, forming tumor thrombi (red arrowhead in L). (M–O) IHC against hIL6. Contrary to control liver (M), majority of the hepatocytes in M were found to highly express hIL6. (O) Hepatocytes in a dysplastic focus (red arrowhead) showing a robust expression of hIL6. (P–R) IHC against PCNA. (P) Control. (Q) PCNA expression was highly positive in the cells in the dysplastic nodule which appears as bulging mass (red arrowheads). (R) The hepatocytes at dysplastic focus (red arrowheads) showed more frequent positivity to PCNA expression than the ones at nondysplastic area (black arrowhead). Bars, 50  $\mu$ m.



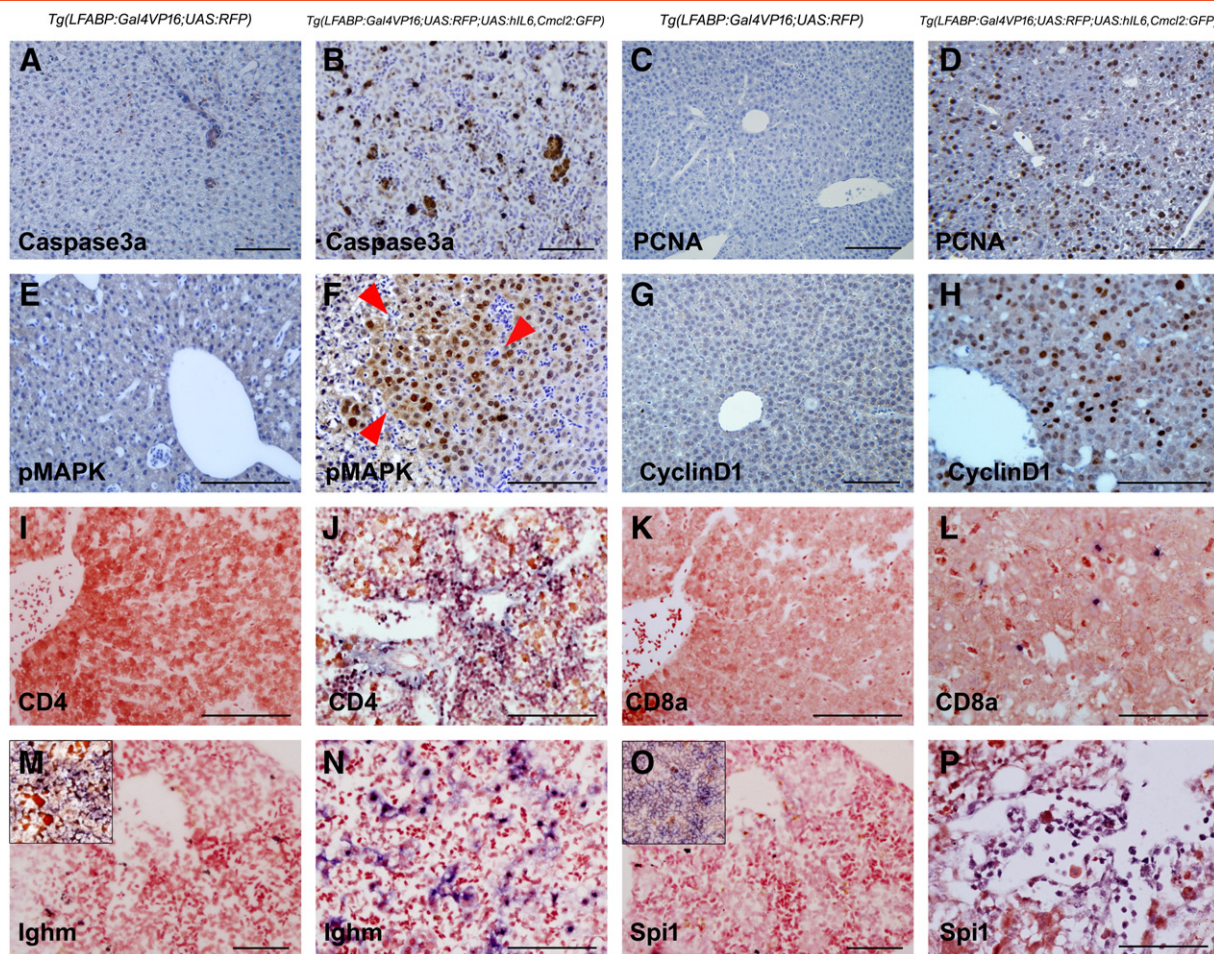


**Figure 4.** hIL6-induced chronic inflammation, cell death, and enhanced proliferation. All images were obtained from 3-month-old zebrafish. (A, C, E, G, I, K, M, and O) Controls. (B) IHC against active caspase 3a showing the positive hepatocytes in the hIL6-expressing liver. (D, F, and H) IHC against proliferation markers PCNA, pMAPK, and cyclin D1, respectively. Note that even the hIL6-expressing liver with nondysplastic foci (D and H) showed marked increase of the marker expression. A dysplastic focus in (F) (red arrowheads) shows a robust positivity for pMAPK. (I–P) ISH for leukocyte markers CD4, CD8a, Ighm, and Spi1. Insets in (M) and (O) indicate zebrafish spleen used as internal control. Majority of the infiltrated T cells are CD4-positive helper T cells. The infiltrated inflammatory cells are located at the portal tract, sinusoids, and intrahepatic vessels. Bars, 50  $\mu$ m.

PI3K/Akt and STAT3 pathways in their HCC zebrafish model but observed no obvious changes. A very recent report with the liver specific expression of oncogenic *kras* gene in zebrafish also showed *in vivo* hepatocarcinogenesis and progression [35]. Expression of the *kras* gene favored a proinflammatory microenvironment which results in the rapid recruitment of neutrophils to oncogenic liver, stimulating HCC. In the present study, our zebrafish model clearly showed the correlation between the chronic inflammation and the occurrence of dysplasia and HCC, which differs from the previous studies. Furthermore, the progression of chronic inflammation and carcinogenesis reflects most of the cellular architectures of the human HCC associated with chronic hepatitis B or C viral infection.

In summary, our study showed that the human IL6 expressed unstably but specifically in the zebrafish liver demonstrated the progression of chronic inflammation and hepatocarcinogenesis. Considering that most of the human HCCs occur through virus-associated chronic inflammation/dysplasia/carcinoma, our current zebrafish model mimics the carcinogenic process occurring in human liver. Further study with the zebrafish model will take more insight into the molecular mechanism of the inflammation-associated hepatocarcinogenesis.

Supplementary data to this article can be found online at <http://dx.doi.org/10.1016/j.neo.2015.07.005>.

## References

- [1] Kaplowitz NK and DeLeve LD (2003). Drug Induced Liver Disease. New York, New York, USA: Marcel Dekker Inc.; 2003 [773 pp.].
- [2] Wong VW, Yu J, and Cheng AS (2009). High serum interleukin-6 level predicts future hepatocellular carcinoma development in patients with chronic hepatitis B. *Int J Cancer* **124**, 2766–2770.
- [3] Hirano T, Yasukawa K, Harada H, Taga T, Watanabe Y, Matsuda T, Kashiwamura S, Nakajima K, Koyama K, and Iwamatsu A (1986). Complementary DNA for a novel human interleukin (BSF-2) that induces B lymphocytes to produce immunoglobulin. *Nature* **324**, 73–76.
- [4] Taub R, Greenbaum LE, and Peng Y (1999). Transcriptional regulatory signals define cytokine dependent and independent pathways in liver regeneration. *Semin Liver Dis* **19**, 117–127.
- [5] Kovalovich K (2001). Interleukin-6 protects against Fas-mediated death by establishing a critical level of anti-apoptotic hepatic proteins FLIP, Bcl-2, and Bcl-xL. *J Biol Chem* **276**, 26605–26613.
- [6] Galun E, Zeira E, Pappo O, Peters M, and Rose-John S (2000). Liver regeneration induced by a designer human IL-6/sIL-6R fusion protein reverses severe hepatocellular injury. *FASEB J* **14**, 1979–1987.



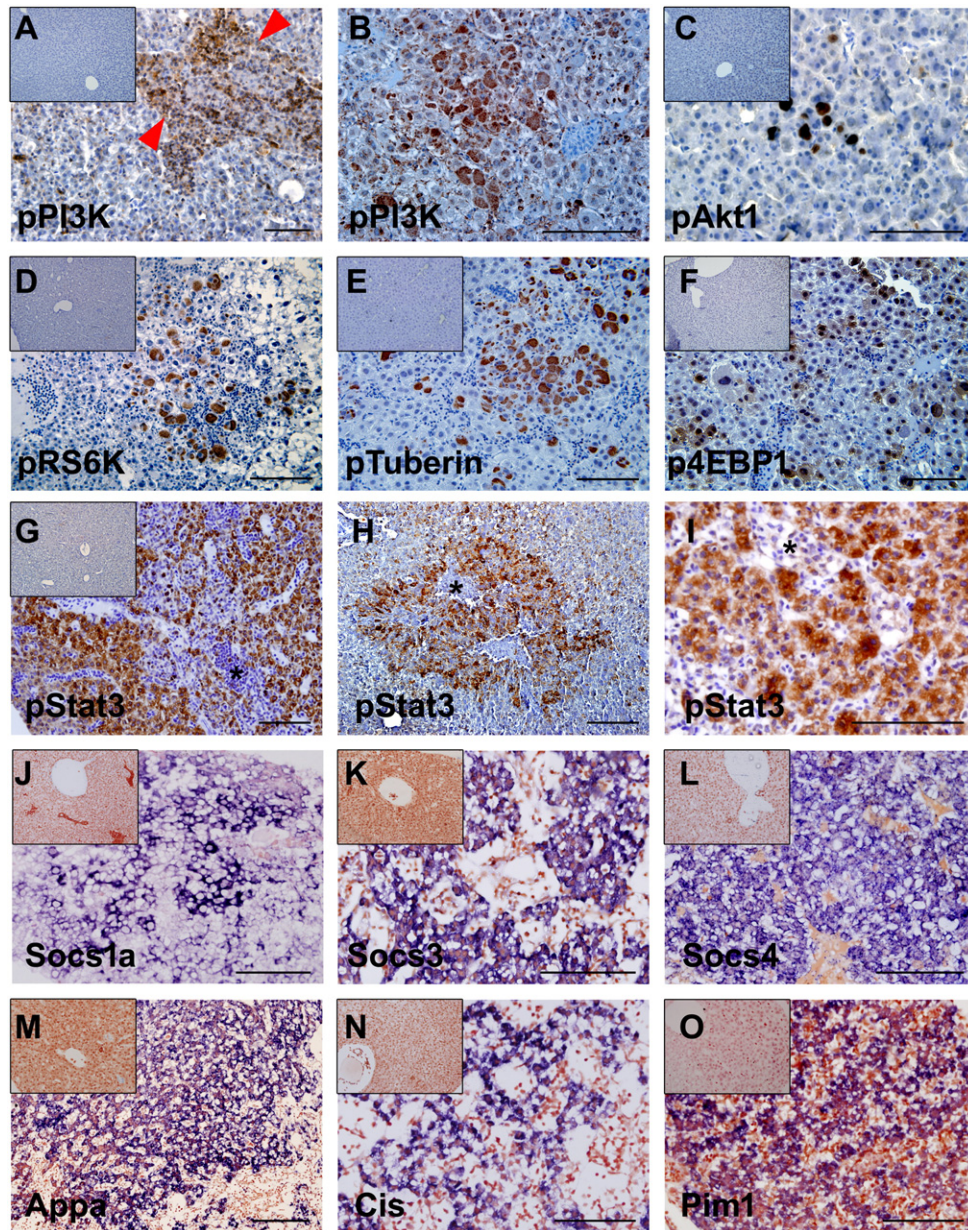


**Figure 5.** IHC and ISH experiments for the molecular components involved in the hIL6-mediated PI3K/Akt and JAK/STAT3 pathways. (A and B, D–H, and J–O) Three-month-old zebrafish. (C and I) Six-month-old zebrafish. (A, H, and L) Inset images are controls. (B–G and I–K) IHC images. (M–P) ISH images. (A and B) IHC against pPI3K. (A) Activated PI3K expression was confined to the infiltrating inflammatory cells in portal area (red arrowheads). (B) Most of the dysplastic foci were negative to the pPI3K except for the hepatocytes with large cell changes. (C–F) IHC for downstream components of the PI3K/Akt pathway. Like the pPI3K expression, expression of the components was restricted to the hepatocytes with large cell change. (G–I) IHC against pSTAT3. Virtually all of the hepatocytes expressing hIL6 were reactive to pSTAT3. (H and I) Robust pSTAT3 expression is seen in a dysplastic focus and HCC, respectively. Note that, contrary to the pPI3K, the infiltrating inflammatory cells (\*) contain negative expression of the pSTAT3. (J–O) ISH for the downstream genes induced by active JAK/STAT3 signaling. Expression of the genes was notably strong in the dysplastic foci. Bars, 50  $\mu$ m.

- [7] Taub R (2003). Hepatoprotection via the IL-6/Stat3 pathway. *J Clin Invest* **112**, 978–980.
- [8] Kuma S, Inaba M, Ogata H, Inaba K, and Okumura T (1990). Effect of human recombinant interleukin-6 on the proliferation of mouse hepatocytes in the primary culture. *Immunobiology* **180**, 235–242.
- [9] Cressman DE, Diamond RH, and Taub R (1995). Rapid activation of the Stat3 transcription complex in liver regeneration. *Hepatology* **21**, 1443–1449.
- [10] Sansone P (2007). IL-6 triggers malignant features in mammospheres from human ductal breast carcinoma and normal mammary gland. *J Clin Invest* **117**, 3988–4002.
- [11] Gao SP, Mark KG, Leslie K, Pao W, Motoi N, Gerald WL, Travis WD, Bornmann W, Veach D, and Clarkson B, et al (2007). Mutations in the EGFR kinase domain mediate STAT3 activation via IL-6 production in human lung adenocarcinomas. *J Clin Invest* **117**, 3846–3856.
- [12] Wustefeld T, Rakemann T, Kubicka S, Manns MP, and Trautwein C (2000). Hyperstimulation with interleukin 6 inhibits cell cycle progression after hepatectomy in mice. *Hepatology* **32**, 514–522.
- [13] Lieschke GJ and Currie PD (2007). Animal models of human disease: zebrafish swim into view. *Nat Rev Genet* **8**, 353–367.
- [14] Liu S and Leach SD (2011). Zebrafish models for cancer. *Annu Rev Pathol* **6**, 71–93.



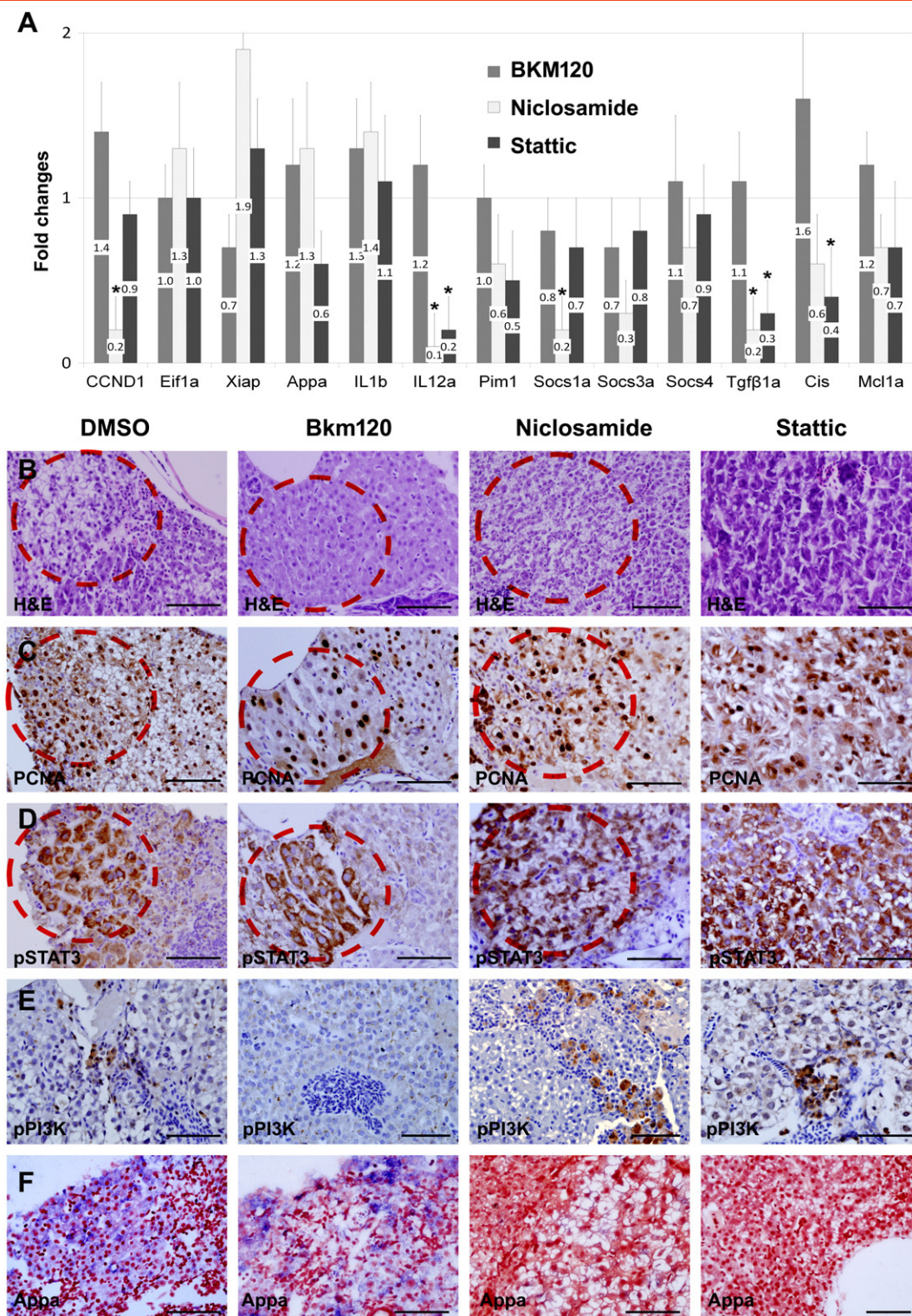


**Figure 6.** Drug inhibition assay on IL6 signaling pathway. (A) Real-time RT-PCR after inhibitor treatment (PI3K inhibitor BKM120 and STAT3 inhibitors Niclosamide and Stattic). Graphs are shown with mean values and standard error bars. The STAT3 inhibitors showed the decreased expression of the downstream components in the JAK/STAT3 pathway. No significant downregulation of the genes in the PI3K/Akt pathway was observed. The asterisk indicates the significant difference between the inhibitor-treated group and the control as determined by Mann-Whitney  $U$  test ( $P < .05$ ). (B) H&E images. (C–E) IHC for PCNA, pSTAT3, and pPI3K after the drug treatment. BKM120 treatment showed downregulation of the pPI3K expression. pSTAT3 expression, however, was not completely suppressed by STAT3 inhibitor treatment. Note that pSTAT3 and PCNA were heavily expressed in the same dysplastic area of serial sections (red circles, sections from the same liver tissue). (F) ISH for Appa showing downregulation by STAT3 inhibitors. Bars, 50  $\mu$ m.

- [15] Lam SH, Wu YL, Vega VB, Miller LD, Spitsbergen J, Tong Y, Zhan H, Govindarajan KR, Lee S, and Mathavan S (2006). Conservation of gene expression signatures between zebrafish and human liver tumors and tumor progression. *Nat Biotechnol* **24**, 73–75.
- [16] Jung IH, Lee GL, Jung DE, and Park SW (2013). Glioma is formed by active Akt1 alone and promoted by active Rac1 in transgenic zebrafish. *Neuro-Oncology* **15**(3), 290–304.
- [17] Her GM, Cheng CH, Hong JR, Sundaram GS, and Wu JL (2006). Imbalance in liver homeostasis leading to hyperplasia by overexpressing either one of the Bcl-2-related genes, zfBclP1 and zfMcl-1a. *Dev Dyn* **235**, 515–523.
- [18] Workman P, Aboagye EO, and Balkwill F (2010). Guidelines for the welfare and use of animals in cancer research. *Br J Cancer* **102**, 1555–1577.
- [19] Park SW, Davison JM, Rhee J, Hruban RH, Maitra A, and Leach SD (2008). Oncogenic KRAS induces progenitor cell expansion and malignant transformation in zebrafish exocrine pancreas. *Gastroenterology* **134**, 2080–2090.
- [20] Jung IH, Jung DE, Park YN, Song SY, and Park SW (2011). Aberrant Hedgehog ligands induce progressive pancreatic fibrosis by paracrine activation of myofibroblasts and ductular cells in transgenic zebrafish. *PLoS One* **6**, 1–15.
- [21] Airaksinen S, Rabergh CMI, Sistonen L, and Nikinmaa M (1998). Effects of heat shock and hypoxia on protein synthesis in rainbow trout (*Oncorhynchus mykiss*) cells. *J Exp Biol* **201**, 2543–2551.
- [22] Katzenellenbogen M, Pappo O, and Barash H (2006). Multiple adaptive mechanisms to chronic liver disease revealed at early stages of liver carcinogenesis in the Mdr2-knockout mice. *Cancer Res* **66**, 4001–4010.
- [23] Kato T, Kameoka S, Kimura T, Nishikawa T, and Kobayashi M (2002). C-erbB-2 and PCNA as prognostic indicators of long-term survival in breast cancer. *Anticancer Res* **22**, 1097–1103.
- [24] Yu H, Pardoll D, and Jove R (2009). STATs in cancer inflammation and immunity: a leading role for STAT3. *Nat Rev Cancer* **9**, 798–809.
- [25] Tilg H, Kaser A, and Moschen AR (2006). How to modulate inflammatory cytokines in liver diseases. *Liver Int* **26**, 1029–1039.
- [26] Tapia-Abellan A, Ruiz-Alcaraz AJ, Hernandez-Caselles T, Such J, Frances R, Garcia-Penarrubia P, and Martínez-Esparza M (2013). Role of MAP Kinases and PI3K-Akt on the cytokine inflammatory profile of peritoneal macrophages from the ascites of cirrhotic patients. *Liver Int* **33**(4), 552–560.
- [27] Morgensztern D and McLeod HL (2005). PI3K/Akt/mTOR pathway as a target for cancer therapy. *Anti-Cancer Drugs* **16**(8), 797–803.
- [28] Molina JR and Adjei AA (2006). The Ras/Raf/MAPK Pathway. *J Thorac Oncol* **1**, 7–9.
- [29] Kiuchi N, Nakajima K, Ichiba M, Fukada T, Narimatsu M, and Mizuno K (1999). STAT3 is required for the gp130-mediated full activation of the c-myc gene. *J Exp Med* **189**, 63–73.
- [30] Buettner R, Mora LB, and Jove R (2002). Activated STAT signaling in human tumors provides novel molecular targets for therapeutic intervention. *Clin Cancer Res* **8**(4), 945–954.
- [31] Li Z, Huang X, Zhan H, Zeng Z, Li C, Spitsbergen JM, and Meierjohann S (2012). Inducible and repressible oncogene-addicted hepatocellular carcinoma in Tet-on xmrk transgenic zebrafish. *J Hepatol* **56**, 419–425.
- [32] Li Z, Zheng W, Wang Z, Zeng Z, Zhan H, Li C, and Zhou L (2013). A transgenic zebrafish liver tumor model with inducible Myc expression reveals conserved Myc signatures with mammalian liver tumors. *Dis Model Mech* **6**, 414–423.
- [33] Nguyen AT, Emelyanov A, Koh CH, Spitsbergen JM, Lam SH, Mathavan S, and Parinov S (2011). A high level of liver-specific expression of oncogenic Kras(V12) drives robust liver tumorigenesis in transgenic zebrafish. *Dis Model Mech* **4**, 801–813.
- [34] Lu JW, Yang WY, Tsai SM, Lin YM, Chang PH, Chen JR, and Wang HD (2013). Liver-specific expressions of HBx and src in the p53 mutant trigger hepatocarcinogenesis in zebrafish. *PLoS One* **8**, e76951.
- [35] Yan C, Huo X, Wang S, Feng Y, and Gong Z (2015). Stimulation of hepatocarcinogenesis by neutrophils upon induction of oncogenic kras expression in transgenic zebrafish. *J Hepatol*. <http://dx.doi.org/10.1016/j.jhep.2015.03.024>.
- [36] Li Z, Luo H, Li C, Huo X, Yan C, Huang X, Al-Haddawi M, Mathavan S, and Gong Z (2004). Transcriptomic analysis of a transgenic zebrafish hepatocellular carcinoma model reveals a prominent role of immune responses in tumour progression and regression. *Int J Cancer* **135**, 1564–1573.